

Theoretical Examination of the 3-[1-(5-Amino-[1,3,4]thiadiazol-2-yl)-2-(1H-imidazol-4-yl)-ethylimino]-2,3-dihydro-indol-2-one Molecule

Efdal ÇİMEN¹ , Veysel TAHİROĞLU^{2*} 

¹ Kafkas University, Kars Vocational School, Chemistry and Chemical Processing Technologies, Kars, Türkiye

² Şırnak University, Health Sciences Faculty, Nursing Department, Şırnak, Türkiye

Efdal ÇİMEN ORCID No: 0000-0003-2461-5870

Veysel TAHİROĞLU ORCID No: 0000-0003-3516-5561

*Corresponding author: veysel.tahiroglu@sirnak.edu.tr

(Received: 18.12.2023, Accepted: 30.03.2024, Online Publication: 28.06.2024)

Keywords

Density functional theory, Molecular electrostatic potential, Natural orbital bonding

Abstract: The vibration frequencies, associated vibrational motions, and theoretically ideal molecular structure of the 3-[1-(5-Amino-[1,3,4]thiadiazol-2-yl)-2-(1H-imidazol-4-yl)-ethylimino]-2,3-dihydro-indol-2-one (1) molecule were investigated using the Gaussian09 software program. The theoretically ideal chemical structure of the molecule (1), its vibration frequencies and the accompanying vibration movements of the molecule were examined. Quantum chemical computations have been performed utilizing the SDD and 6-311G base set of DFT(RB3LYP) methods. The molecule was subjected to the highest occupied molecular orbital (HOMO), the lowest unoccupied molecular orbital (LUMO) investigations to ascertain charge transfer. The molecule's stability was investigated using Natural Orbital Bonding (NBO) analysis as a function of both hyperconjugative interaction and charge delocalization. Molecular Electrostatic Potential (MEP) was performed using a Density Functional Theory (DFT) technique. Both estimated DFT algorithms have comparable geometric parameters.

6

3-[1-(5-Amino-[1,3,4]tiadiazol-2-il)-2-(1H-imidazol-4-il)-etilimino]-2,3-dihidro-indol-2-on Molekülün Teoriksel İncelenmesi

Anahtar Kelimeler

Yoğunluk fonksiyonel teorisi, Moleküler elektrostatik potansiyel, Doğal orbital bağlanma

Öz: 3-[1-(5-Amino-[1,3,4]tiadiazol-2-il)-2-(1H-imidazol-4-il)-etilimino]-2,3-dihidro-indol-2-on (1) molekülünün titreşim frekansları, ilişkili titreşim hareketleri ve teorik olarak ideal moleküler yapısı Gaussian 09 yazılım programı kullanılarak araştırıldı. Molekül (1)'in teorik olarak ideal kimyasal yapısı, titreşim frekansları ve molekülün buna eşlik eden titreşim hareketleri incelenmiştir. Kuantum kimyasal hesaplamalarını gerçekleştirmek için DFT(RB3LYP) yaklaşımlarının SDD ve 6-311G temel seti kullanıldı. Moleküldeki yük aktarımı için en yüksek dolu moleküler yörünge (HOMO), en düşük boş moleküler yörünge (LUMO) analizleri yapılmıştır. Molekülün stabilitesi, hem hiperkonjugatif etkileşimin hem de yük delokalizasyonunun bir fonksiyonu, Doğal Orbital Bağlanma (NBO) analizi kullanılarak araştırıldı. MEP, bir Yoğunluk fonksiyonel teorisi (DFT) tekniği kullanılarak gerçekleştirildi. Tahmin edilen her iki DFT algoritması da karşılaştırılabilir geometrik parametrelere sahiptir.

1. INTRODUCTION

The azomethine group, often referred to as the imine functional group, is a component of Schiff base derivatives, which are compounds that have become more well-known due to their biological activity, including antibacterial, anticancer, antifungal, and antimicrobial qualities [1]. These substances represent the largest class of photochromic materials with potential for use in optoelectronic devices. In recent years,

potential applications have focused on the electrochemical characteristics and nonlinear optical (NLO) behavior of Schiff base ligands with various substituents that have different electron-donating and electron-withdrawing groups [2]. Furthermore, because of their selectivity, synthetic flexibility and sensitivity to transition metal ions, The ligands of Schiff bases are important in inorganic alchemy [3]. Schiff bases metal complexes produced from heterocyclic compounds with ligand atoms of nitrogen, oxygen, and sulfur are employed in therapeutic and pharmaceutical applications

[4]. Thiophene and its derivatives play an essential role in heterocyclic chemistry. They are utilized as charge-carrying molecules in technologies such as transistors, supercapacitors, Electrochromic substances, chemical solar panels, and organic light-emitting diodes, and nonlinear optical materials [5]. In recent years, potential applications have focused on the electrochemical characteristics and nonlinear optical (NLO) behavior of Schiff base ligands with various substituents that have different groups that donate electrons and groups that remove electrons [6]. Physical and chemical characteristics of chemical and biological systems may now be predicted because to advances in computational chemistry. Furthermore, theoretical considerations substantially aid actual spectroscopic research. Density Functional Theory (DFT) is widely used in computing the UV-Vis, FT-IR, and NMR spectra, charge distributions, HOMO-LUMO energies, and nonlinear optical (NLO) behavior of certain thiophene derivatives. Such substances have shown reliable findings that are compatible with experimental data [7].

The quantum chemical model of matter is known as density functional theory (DFT). Physicists, chemists, and materials workers prefer this model because simulation results are comparable to experimental studies. It reduces simulation time without affecting accuracy by considering the collective effect of electrons [8]. This is different from other models accepted in scientific studies. Thomas (1927) and Fermi (1928) also helped solve the many-electron problem in the years when the Hartree and Hartree-Fock methods emerged. Thomas and Fermi proposed the original density functional theory of quantum systems. This method explains how density functional theory (DFT) works, but is not precise enough for modern electronic structure calculations [9].

2. MATERIAL AND METHOD

DFT was calculated using the (B3LYP)/SDD and 6-311G techniques using Gaussian 09 software. For conformational analysis, a quasi-experimental approach is used. The form of the final molecule was optimized as the initial stage in the computer study. The vibrational frequencies, optimal geometries, and energies of molecular structure of the molecule (1) have been calculated utilizing the DFT approach in the Gaussian 09 software. The DFT/(B3PW91/B3LYP) approaches and the 6-311G base set based software package have been used to develop the Lee's-Yang-Parr correlation function. ChemBio Ultra Drive 3D and GaussView

6.0.16 were used to capture the visualization and input file [10]. The binding affinity of the molecule was calculated using the Maestro Molecular Modeling platform and the Schrödinger, LLC model (model 6.0.16.) [11]. This experiment made use of the Gaussian 09W package software. To do theoretical computations on the examined chemical, the Density Functional Theory (DFT) technique was performed. The DFT computations utilized the B3LYP mixed functional, which consists of Becke's three-parameter exchange functional and Lee, Yang, and Parr's correlation functional and is one of the most widely used exchange-correlation functionals [12]. SDD and 6-311G base sets have been used to achieve geometry optimizations, geometric parameters, and minimal molecular energies of the molecule. Mulliken charges, molecular electrostatic potential surfaces and frontier orbitals have been calculated utilizing the B3LYP/SDD/6-311G method. However, using the same procedure, LUMO and HOMO energies of the molecule (1) were calculated and ΔE energy differences were obtained for each method using these data.

3. RESULTS AND DISCUSSION

3.1. Structure Details and Analysis

A molecule's geometry is related to the bond angle and bond length between the atoms of that molecule and is one of the most important factors that directly affects the magnitude of the molecule's the dipole moment [13]. The B3LYP method with SDD and 6-311G basis sets was utilized for geometric optimization computations to explore the the molecule (1) influence of the DFT technique on geometric features. Some angles bonding and lengths bonding of the molecule (1) obtained by the help of the Gaussian 0.9 program are given in Table 1 [14]. The largest deviation appears in the C14-S15 structural by a bond length of 1.84342 Å. Another structure with the largest deviation appears in the C12-C13 structural by a bond length of 1.57546 Å. This is because there are N and O atoms, which are strong electron-withdrawing groups, attached to the C8 atom. The largest deviation in trihedral structures was determined in the N7-C8-O10 structure with the bond angle of 125.85439°. In tetrahedral structures, The bond angle between C16-S15-C14-N18 was found to have the greatest variation, 1.15446°. The lowest change in bond length in the C2-H26 structure was determined to be -0.00568 Å. The smallest change in bond angle in trihedral structures is N7-C8-O10 -17.33484 and N11-C12-C13-C20 -0.04996, respectively.

Table 1. Theoretically determined some bond lengths (Å) and angles (°) of the molecule (1).

Bond Lengths	B3LYP/ SDD	B3LYP/ 6-311G	Bond Lengths	B3LYP/ SDD	B3LYP/ 6-311G
C1-C2	1.41136	1.39999	C12-H30	1.09577	1.08991
C3-C4	1.39675	1.38731	C13-H32	1.09525	1.08899
C5-C6	1.39944	1.38960	C22-H35	1.07906	1.07388
C5-C9	1.47519	1.46960	C4-N7	1.42102	1.41565
C8-C9	1.54551	1.53122	C9-N11	1.29193	1.28326
C12-C13	1.57546	1.56918	C16-N19	1.37067	1.35878
C12-C14	1.50288	1.49309	C22-N21	1.33629	1.32775
C13-C20	1.49968	1.49095	N17-N18	1.40712	1.40407
C20-C24	1.39034	1.37705	C8-O10	1.25112	1.24445
C2-H26	1.08736	1.08168	C14-S15	1.84342	1.84935
Bond Angles	B3LYP/ SDD	B3LYP/ 6-311G	Bond Angles	B3LYP/ SDD	B3LYP/ 6-311G
C1-C2-C3	121.43395	121.43000	C1-C6-H28	121.50067	121.57496
C3-C4-C5	121.85055	121.74364	H31-C13-H32	108.51955	108.31528
C5-C9-C8	105.39422	105.54416	N7-C8-O10	108.51955	125.85439
C12-C13-C20	112.58595	112.98100	C14-S15-C15	84.25298	83.96123
C4-N7-C8	111.97479	112.02741	N18-N17-C16	112.25886	112.68447
Planar Bond Angles	B3LYP/ SDD	B3LYP/ 6-311G	Planar Bond Angles	B3LYP/ SDD	B3LYP/ 6-311G
C3-C2-C1-C6	-0.00748	0.00085	N21-C22-N23-C24	-0.00094	-0.02212
C4-C5-C9-C8	0.90158	1.09487	C16-S15-C14-N18	1.06657	1.15446
C4-N7-C8-C9	0.88384	1.07379	N11-C12-C13-C20	-179.06379	-179.11375
N11-C9-C8-O10	-2.79432	-3.23090	O10-C8-N7-H29	0.81900	0.76218

3.2. Mulliken Atomic Charges

Atomic charge is utilized to predict electrostatic potentials across molecule boundaries, evaluate charge transfer, and evaluate electronegativity equalization [15]. Mulliken atomic charges of the molecule (1) The gas phase were determined using the B3LYP theory SDD basis set and B3LYP theory 6-311G basis set and are given in Table 2 [16]. It has been noted that the

electronegative atoms (N7, N11, N17, N18, N21, N23 and O10) in the molecule have negative charge values. The charge values of these atoms are; It was calculated as -0.447, -0.004, -0.104, -0.058, -0.116, -0.321 and -0.263 (a.u.). Utilizing the RB3LYP procedure with the 6-311G base set, a) bond lengths, b) mulliken charge, c) structure optimization d) atomic mass are given in Figure 1 [16].

Table 2. Mulliken atomic charges of the molecule (1).

	B3LYP/ SDD	B3LYP/ 6-311G		B3LYP/ SDD	B3LYP/ 6-311G
C1	-0.233	-0.183	N7	-0.447	-0.834
C2	-0.173	-0.130	N11	-0.004	-0.251
C3	-0.343	-0.067	N17	-0.104	-0.261
C4	0.279	0.332	N18	-0.058	-0.180
C5	0.193	-0.181	N21	-0.116	-0.367
C6	-0.340	0.003	N23	-0.321	-0.321
C8	0.115	0.559	S15	0.237	0.279
C9	-0.145	0.000	H26	0.224	0.155
C12	-0.150	-0.268	H27	0.234	0.170
C13	-0.467	-0.372	H28	0.265	0.187
C14	-0.133	0.065	H30	0.289	0.250
C16	-0.135	-0.228	H31	0.221	0.200
C20	0.238	-0.006	H34	0.335	0.344
C22	-0.235	0.224	H35	0.257	0.196
C24	-0.342	0.182	H36	0.210	0.336
O10	-0.263	-0.382	H37	0.287	0.210

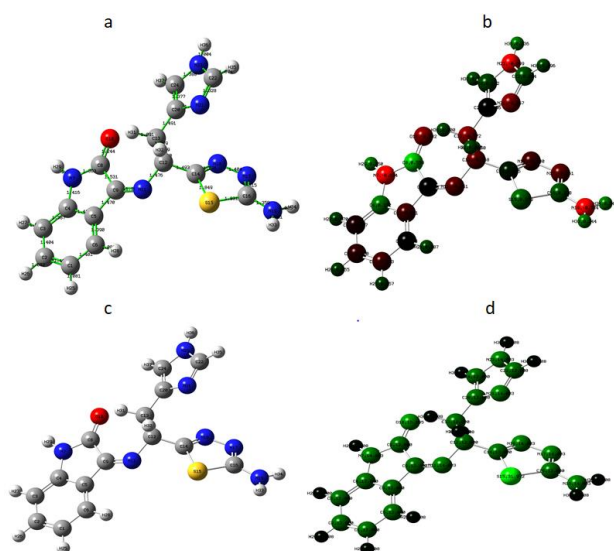


Figure 1. Molecule with DFT/B3LYP/6-311G basis set (1) a) bond lengths, b) relative charge, c) structure optimization d) atomic mass.

3.3. HOMO and LUMO Analysis

The lowest unoccupied molecular orbital (LUMO) and the highest occupied molecular orbital (HOMO) are very significant two orbitals in molecules [17]. The eigenvalues and gap energies of LUMO and HOMO represent the bioactivity of a chemical [18]. A chemical with a short gap between its border orbitals is more polarizable and has lower kinetic stability and increased chemical reactivity [19]. Because the HOMO, being the outside orbital holding electrons, tries to transfer electrons as electron donors, the HOMO's energy directly impacts the ionization potential. Although, LUMO might receive electrons, and its energy is proportional to its electron affinities [20]. The eigenvalues and energy deficits of HOMO and LUMO chemicals indicate the molecule's biological activity. Two key chemical orbitals have been studied for the HOMO and LUMO energies, as illustrated in Figures 2 and 3 [21]. In the Table 3 [22] is shown the computed quantum chemical factor (in eV) for low energy suitability of molecule (1) using DFT/B3LYP/SDD and DFT/B3LYP/6-311G techniques.

The orbital energies of LUMO and HOMO might be used to calculate electron affinity and ionization energy as follows: $A = -E_{LUMO}$, $I = -E_{HOMO}$, $(\mu = -(I+A)/2)$ and $\eta = (I-A)/2$. An electrophilic system is one that resists transferring electrons with its surroundings and can store more electrons than a non-electrophilic system [23]. It is a more accurate indicator of total chemical reactivity since it includes data on durability (hardness) as well as electron transfer (Potential chemical). The affinity of electrons and potential for ionization are the chemical species, and the formulas $\eta = (I-A)/2$ and $\mu = -(I+A)/2$ are used

to calculate the chemical potential and hardness, respectively (A) [24]. The components from which the title compound is created do not spontaneously dissolve because of the complex's stable and negative chemical potential, which results from its negativity. The stiffness of an electron nebula in a chemical structure is its resistance to distortion caused by minor perturbations during chemical processing. Hardness is a notion used in physics and chemistry, although it cannot be seen physically. Though soft systems can be substantially and highly polarized, hard systems are less polarized and often tiny [25].

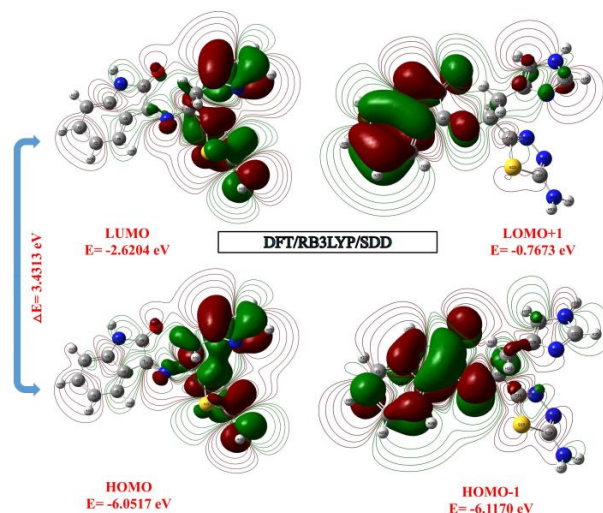


Figure 2. Boundary molecular orbitals of the molecule (1) as per the DFT/B3LYP/SDD phase.

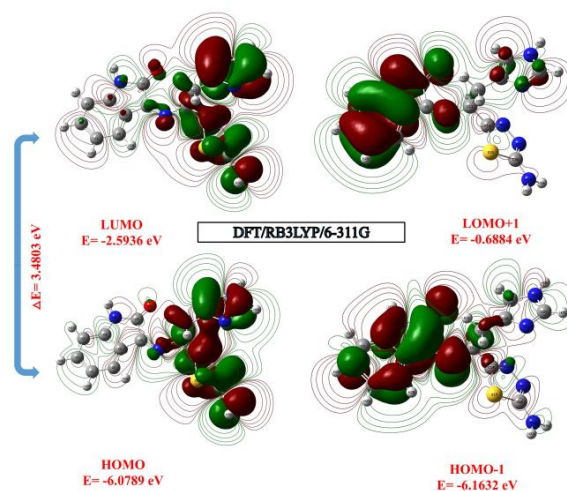


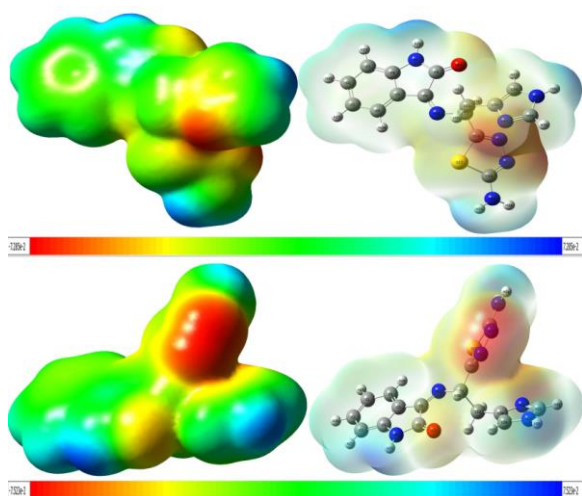
Figure 3. Boundary molecular orbitals of the molecule (1) as per the DFT/B3LYP/6-311G level.

Table 3. Calculated quantum chemical parameters*(in eV) to low energy compatibilities by DFT/RB3LYP/SDD-DFT/RB3LYP/6-311G methods of the molekül (1).

Molecules Energy		DFT/ B3LYP SDD	DFT/B3LYP 6-311G
E_{LUMO}		-2.6204	-2.5986
E_{HOMO}		-6.0517	-6.0789
E_{LUMO+1}		-0.7673	-0.6884
E_{HOMO-1}		-6.1170	-6.1632
Energy Gap	$(\Delta E)E_{HOMO} - E_{LUMO}/$	3.4313	3.4803
Ionization Potential	$(I = -E_{HOMO})$	6.0517	6.0789
Electron Affinity	$(A = -E_{LUMO})$	2.6204	2.5986
Chemical hardness	$(\eta = (I - A)/2)$	1.7156	1.7401
Chemical softness	$(s = 1/2 \eta)$	0.8578	0.8700
Chemical Potential	$(\mu = -(I + A)/2)$	-4.3360	-4.3387
Electronegativity	$(\chi = (I + A)/2)$	1.8102	1.7993
Electrophilicity index	$(\omega = \mu^2/2 \eta)$	5.4793	5.4089

3.4. Molecular Electrostatic Potential (MEP)

MEP may be used to describe hydrogen bond interactions in addition to electrophilic and nucleophilic activities. It has been correlated with electron density (ED) [26]. The electrostatic potential $V(r)$ is highly appropriated to research procedures requiring molecular identification, like interactions between receptors and drugs and enzymes and substrates. Because these two species initially perceive one other through the lens of their potential [27]. The electrophilic and nucleophilic portions of the examined compound have been predicted utilising the B3LYP/SDD and B3LYP/6-311G basis sets utilizing MEP in optimal geometry. As demonstrated in Figure 4 [28], MEP's negative (yellow or red) regions show electrophilic reacting, whereas favorable (blue) areas represent nucleophilic reactivity.

**Figure 4.** Molecular electrostatic potential field of molecule (1) utilising DFT/B3LYP and DFT/B3LYP methods with SDD and 6-311G basis set.

3.5. Non-Linear Optical Properties (NLO)

Nonlinear optical characteristics (NLO) are computationally predicted using polarizability (α) and hyperpolarizability (β) values [29]. Polarizability defines optical characteristics in organic-based materials. The hyperpolarizability of a material impacts the performance of its nonlinear optical characteristics. To show NLO qualities, a molecule's polarizability, hyperpolarizability, and dipole moment must be high, and the HOMO-LUMO energy difference must be modest [30]. Using the B3LYP/SDD(d,p) and B3LYP/6-311G method and basis sets, the hyperpolarization (β), polarization (α), and electric dipole moment (μ) of the molekül (1), NLO activity were measured. In the Table 4 [31] has been showed the calculated NLO values. The mean values of the polarizability (α), static dipole moment (μ), and total first static hyperpolarizability (β) of the x, y, and z components have been obtained from equations Equality 1-4." The total values molecule (1) determined using the DFT/B3LYP/SDD and DFT/B3LYP/6-311G methods are 3.48×10^{-30} esu and 3.55×10^{-30} esu, respectively.

$$\mu = (\mu_x^2 + \mu_y^2)^{1/2} \quad (1)$$

$$\alpha = 2^{-1/2} [(\alpha_{xx} - \alpha_{yy})^2 + (\alpha_{yy} - \alpha_{zz})^2 + (\alpha_{zz} - \alpha_{xx})^2 + 6\alpha_{xx}^2]^{1/2} \quad (2)$$

$$\beta_{Total} = (\beta^2x + \beta^2y + \beta^2z)^{1/2} \quad (3)$$

$$= [(\beta_{xxx} + \beta_{xyy} + \beta_{xzz})^2 + (\beta_{yyy} + \beta_{yxx} + \beta_{yzz})^2 + (\beta_{zzz} + \beta_{zxx} + \beta_{zyy})^2]^{1/2} \quad (4)$$

Table 4. The dipole moments (Debye), polarizability (au), components, and total value of molecule (1) are computed using the SDD and 6-311G basis sets using the DFT/B3LYP technique.

Parameters	B3LYP/ SDD	B3LYP/ 6-311G	Parameters	B3LYP/ SDD	B3LYP/ 6-311G
μ_x	-3.1262	-2.6959	β_{xxx}	-41.5112	-19.4581
μ_y	-0.3183	-0.4954	β_{yyy}	42.6236	37.5772
μ_z	-0.9230	-0.7217	β_{zzz}	1.8263	3.7207
$\mu(D)$	3.2751	2.8344	β_{xyy}	124.3641	126.6830
α_{xx}	-101.7798	-102.7201	β_{xxy}	-39.9238	-37.7491
α_{yy}	-113.3843	-114.9895	β_{xxz}	9.7610	14.4029
α_{zz}	-157.9199	-157.9704	β_{xzz}	-22.5224	-21.2227
α_{xy}	2.9098	3.0128	β_{yzz}	-0.7940	-0.7190
α_{xz}	-3.0550	-2.7397	β_{yyz}	0.7671	2.6970
α_{yz}	-10.5986	-9.3997	β_{xyz}	-1.8619	0.8662
α (au)	-185.172	-184.8441	β (esu)	3.48×10^{-30}	3.55×10^{-30}

3.6. NBO Analysis

To better understand the intermolecular interactions of our compound, NBO analysis was performed on the optimized structures [32]. The NBO analysis software from the Gaussian 09W program package was utilized. The DFT (B3LYP) approach is used in the comparisons in the Table 5 [33] to demonstrate the percentages of individual bond electrons for and bonds in distinct bonds, as well as variations in the percentages of electrons in s,

p, and d orbitals on each atom. A quadratic is used for molecule (1). Fock matrix was used to forecast the relationship between the receiver (j) and the donor (i). The stabilizing value associated with delocalization is projected to be as follows Equality 5 to every donor (i) and recipient

$$E(2) = \Delta E_{ij} = q_i \frac{(F_{i,j})^2}{(\epsilon_i - \epsilon_j)} \quad (5)$$

The NBO element of the Fock matrix is $F(i,j)$, the diagonal elements are i and j , and the donor orbital occupancy is q_i . The higher the stabilization energy, the more electrons are likely to be transferred to acceptor orbitals [2]. The electron density, $E(2)$, $E(j)-E(i)$, and $f(i,j)$ values, as well as NBO computations, are shown in Table 5 [33] for a few chosen donors and acceptors. The interplay between the stabilization energy $E(2)$, full and unfilled NBO type Lewis orbitals, and electron delocalization from bonding (BD) to antibonding (BD*) orbitals is characterized by NBO analysis. Bond (σ/π) and anti-bond (σ^*/π^*) interactions also contribute considerably to structural stability, with the $\pi(C5-C6)/\pi^*(C3-C4)$ interaction having the highest E value of 30.17 kcal/mol. (2), followed by the $\pi(C1-C2)/\pi^*(C5-C6)$ interaction with 7.54 kcal/mol.

Table 5. Selected NBO results of molecule (1) are computed set using the DFT/B3LYP technique and the SDD basis set.

NBO(i)	Type	Occupancies	NBO(j)	Type	Occupancies	$E(2)^a$ (Kcal/mol)	$E(j)-E(i)^b$ (a.u.)	$F(i,j)^c$ (a.u)
C1-C2	σ	1.98122	C1-C6	σ^*	0.01327	1.42	1.22	0.037
C1-C6	σ	1.97809	C1-H25	σ^*	0.01442	0.71	1.20	0.026
C1-C2	π	1.66611	C5-C6	π^*	0.35889	22.55	0.29	0.072
C2-C3	σ	1.97584	C4-N7	σ^*	0.02889	7.11	1.05	0.077
C3-C4	π	1.66701	C1-C2	π^*	0.33082	22.19	0.29	0.072
C4-C5	σ	1.96039	C9-N11	σ^*	0.01657	4.61	1.26	0.068
C5-C6	π	1.64491	C3-C4	π^*	0.37349	24.68	0.27	0.074
C6-H28	σ	1.97628	C1-C2	σ^*	0.01546	4.67	1.05	0.063
C8-C9	σ	1.97087	C5-C6	σ^*	0.02306	5.61	1.19	0.073
C8-O10	π	1.97119	C9-N11	π^*	0.14278	0.63	0.39	0.043
C9-N11	π	1.88665	C8-O10	π^*	0.29819	12.18	0.30	0.057
C5-C6	π	1.64491	C9-N11	π^*	0.14278	18.13	0.26	0.065
C13-H32	σ	1.97613	C20-C24	σ^*	0.03128	5.94	1.04	0.070
C14-S15	σ	1.97035	C16-N19	σ^*	0.02406	5.55	1.04	0.068
C14-N18	π	1.93607	C16-N17	π^*	0.39043	7.77	0.31	0.048
C16-N17	π	1.90315	C14-N18	π^*	0.26756	12.27	0.32	0.059
N17-N18	σ	1.97117	C12-C14	σ^*	0.03547	5.47	1.17	0.072
N19-H34	σ	1.98397	S15-C16	σ^*	0.09479	5.68	0.78	0.061
C20-C24	π	1.82681	N21-C22	π^*	0.37577	16.39	0.26	0.061
N21-C22	π	1.87079	C20-C24	π^*	0.31090	21.22	0.33	0.078
C22-H35	σ	1.98014	C20-N21	σ^*	0.02637	4.77	0.98	0.061
N23-C24	σ	1.98435	C13-C20	σ^*	0.02161	5.78	1.21	0.075
C20-C24	σ	1.97960	C13-H31	σ^*	0.01500	0.96	0.44	0.046
C22-N23	σ	1.99080	C24-H37	σ^*	0.01152	2.84	1.32	0.055
N23-C24	σ	1.98435	C13-C20	σ^*	0.02161	5.78	1.21	0.075
N23-C24	σ	1.98435	C22-H35	σ^*	0.01802	2.88	1.29	0.054
N23-H36	σ	1.99062	C20-C24	σ^*	0.03128	1.92	1.26	0.044
C24-H37	σ	1.98165	C22-N23	σ^*	0.03752	3.76	0.95	0.054

4. CONCLUSION

Important geometric data like as bond angles and bond lengths of the structure's atoms were gathered as a consequence of molecular optimization. The B3LYP/6-31G and B3LYP//SDD techniques were used to calculate the different (E) between the compound's HOMO and LUMO energy levels depending on the solvent. The energy different between LUMO and HOMO did not vary importantly as the solvent polarity rose, implying that the solvent polarity had no influence on the contact of the chemical and the creation of the action. The Mulliken charge distribution method was used to collect information on the charge distribution on the atoms as well as the various features of the molecular structures. Furthermore, the MEP map discovered by employing the compound's DFT/RB3LYP/6-31G and DFT/B3LYP/SDD base sets The area has been discovered to be surrounding the methyl and hydrogen atoms, and these properties supplied us with knowledge about the regions of the chemical where non-covalent interactions may occur.

REFERENCES

- [1] Taslimi P, et al. Metal contained Phthalocyanines with 3,4-Dimethoxyphenethoxy substituents: their anticancer, antibacterial activities and their inhibitory effects on some metabolic enzymes with molecular docking studies. *Journal of Biomolecular Structure and Dynamics*, 2022; 40(7): p. 2991-3002.
- [2] Ulaş Y. 2-((1H-indol-1-il)(naftalen-1-il)metil)fenol Bileşiğinin Sentezi ve NLO Özelliklerinin Quantum Kimyasal Hesaplamalarla İncelenmesi. *Caucasian Journal of Science*. 2022; 9(2): p. 184-195.
- [3] Liu X. and J.-R Hamon. Recent developments in penta-hexa- and heptadentate Schiff base ligands and their metal complexes. *Coordination Chemistry Reviews*. 2019; 389: p. 94-118.
- [4] Abu-Dief A.M. and Mohamed I.M.A. A review on versatile applications of transition metal complexes incorporating Schiff bases. *Beni-Suef University Journal of Basic and Applied Sciences*, 2015; 4(2): p. 119-133.
- [5] Betiha M.A, et al. Oxidative desulfurization using graphene and its composites for fuel containing thiophene and its derivatives. *Egyptian Journal of Petroleum*. 2018; 27(4): p. 715-730.
- [6] Cowan R.D. Theoretical Calculation of Atomic Spectra Using Digital Computers. *Journal of the Optical Society of America*. 1968; 58(6): p. 808-818.
- [7] Karakurt T. 3-[(E)-2-(4-fenil-1,3-tiyazol-2-yl)hidrazin-1-yiliden]-indolin-2-on Bileşiğinin Tautomer Yapısı Üzerinde Gaz ve Katı Fazında Teorik Hesaplamalar. *Afyon Kocatepe Üniversitesi Fen Ve Mühendislik Bilimleri Dergisi*. 2020; 20(1): p. 96-102.
- [8] Michael J. Frisch B.S. Gustavo Scuseria, Mike Robb, Richard Cheeseman Jr, Giovanni Scalmani, Barone villagrande, Benedetta Mennucci, Gaussian 09, in gaussian. Inc., Wallingford. 2009.
- [9] Callaway J. and N.H March. *Density Functional Methods: Theory and Applications*, in Solid State Physics. H. Ehrenreich, D. Turnbull, and F. Seitz, Editors. 1984; Academic Press. p. 135-221.
- [10] Tanriverdi A.A, et al. Structural and Spectral Properties of 4-(5-methyl-[1,2,4] triazolo [1,5-a] pyrimidine-7-yloxy) phthalonitrile: Analysis by TD-DFT Method, ADME Analysis, and Molecular Docking Simulations. *Journal of the Institute of Science and Technology*. 2022; 12(4): p. 2340-2351.
- [11] Kökbudak Z, Türkmenoğlu B, and Akkoç S. A New Schiff Base Molecule Prepared from Pyrimidine-2-thione: Synthesis, Spectral Characterization, Cytotoxic Activity, DFT, and Molecular Docking Studies. *Adiyaman University Journal of Science*. 2022; 12(1): p. 9-25.
- [12] Abu-Awwad F, and Politzer P. Variation of parameters in Becke-3 hybrid exchange-correlation functional. *Journal of Computational Chemistry*. 2000; 21(3): p. 227-238.
- [13] Gören K, Bağlan M, and Çakmak İ. Theoretical Investigation of ¹H and ¹³C NMR Spectra of Diethanol Amine Dithiocarbamate RAFT Agent. *Journal of the Institute of Science and Technology*. 2022; 12(3): p.1677-1689.
- [14] Yüksek H, et al. B3LYP ve HF Temel Setleri Kullanılarak Bazı 3-Alkil-4-(2-asetoksi-3-metoksibenzilidenamino)-4,5-dihidro-1H-1,2,4-triazol5-on Bileşiklerinin Deneysel ve Teorik Özelliklerinin İncelenmesi. *Celal Bayar University Journal of Science*. 2017; 13(1): p.193-204.
- [15] Bağlan M, Gören K, and Yildiko Ü. DFT Computations and Molecular Docking Studies of 3-(6-(3-aminophenyl)thiazolo[1,2,4]triazol-2-yl)-2H-chromen-2-one(ATTC) Molecule. *Hittite Journal of Science and Engineering*. 2023; 10(1): p. 11-19.
- [16] Beytur M, and Yüksek H. 3-Fenil-4-(3-Sinnoiloksibenzilidenamino)-4,5-Dihidro-1H-1,2,4-Triazol-5-On Molekülünün Spektroskopik Özellikleri. *Caucasian Journal of Science*. 2018; 5(2): p. 65-80.
- [17] Bağlan M., Gören K, and Yildiko Ü. HOMO–LUMO, NBO, NLO, MEP analysis and molecular docking using DFT calculations in DFPA molecule. *International Journal of Chemistry and Technology*. 2023; 7(1): p. 38-47.
- [18] Mumit M.A, et al. DFT studies on vibrational and electronic spectra, HOMO–LUMO, MEP, HOMA, NBO and molecular docking analysis of benzyl-3-N-(2,4,5-trimethoxyphenylmethylene)hydrazinecarbodithioat e. *Journal of Molecular Structure*. 2020; 1220: p.128715.
- [19] Bağlan M, Yildiko Ü, and Gören K. DFT Calculations And Molecular Docking Study In 6-(2-Pyrrolidinone-5-Yl) Epicatechin Molecule From Flavonoids. *Eskişehir Teknik Üniversitesi Bilim ve Teknoloji Dergisi B - Teorik Bilimler*. 2023; 11(1): p. 43-55.

- [20] Brownell L.V, et al. Highly Systematic and Efficient HOMO–LUMO Energy Gap Control of Thiophene-Pyrazine-Acenes. *The Journal of Physical Chemistry C*. 2013; 117(48): p. 25236-25247.
- [21] Jiang D, and Dai S. Circumacenes versus periacenes: HOMO–LUMO gap and transition from nonmagnetic to magnetic ground state with size. *Chemical Physics Letters*. 2008; 466(1): p. 72-75.
- [22] Zhang T, et al. Clarifying the Adsorption of Triphenylamine on Au(111): Filling the HOMO–LUMO Gap. *The Journal of Physical Chemistry C*. 2022; 126(3): p. 1635-1643.
- [23] Choudhary V, et al. DFT calculations on molecular structures, HOMO–LUMO study, reactivity descriptors and spectral analyses of newly synthesized diorganotin(IV) 2-chloridophenylacetohydroxamate complexes. *Journal of Computational Chemistry*. 2019; 40(27): p. 2354-2363.
- [24] Zhuo L, Liao G.W, and Yu Z. A Frontier Molecular Orbital Theory Approach to Understanding the Mayr Equation and to Quantifying Nucleophilicity and Electrophilicity by Using HOMO and LUMO Energies. *Asian Journal of Organic Chemistry*. 2012; 1(4): p. 336-345.
- [25] Pereira F, et al. Machine Learning Methods to Predict Density Functional Theory B3LYP Energies of HOMO and LUMO Orbitals. *Journal of Chemical Information and Modeling*. 2017; 57(1): p. 11-21.
- [26] Bağlan M., Yıldiko Ü, and Gören K. Computational Investigation of 5,5-trihydroxy-3,7-dimethoxy-4-O-biflavone from Flavonoids Using DFT Calculations and Molecular Docking. *Adıyaman University Journal of Science*. 2022; 12(2): p. 283-298.
- [27] Uysal Ü.D, Berber H, and Aydoğdu Erdönmez A. 2-Etoksi-6-[(E)-(2-Hidroksifenil)imino]metil]fenol Türevi Schiff Bazlarının Sentezi ve Teorik Çalışmalar. *Süleyman Demirel Üniversitesi Fen Bilimleri Enstitüsü Dergisi*. 2020; 24(2): p. 419-431.
- [28] Luque F.J, et al. SCRF calculation of the effect of water on the topology of the molecular electrostatic potential. *The Journal of Physical Chemistry*. 1993; 97(37): p. 9380-9384.
- [29] Öztürk N, et al. Structural, Spectroscopic (FT-IR, Raman and NMR), Non-linear Optical (NLO), HOMOLUMO and Theoretical (DFT/CAM-B3LYP) Analyses of N-Benzyloxycarbonyloxy-5-Norbornene-2,3-Dicarboximide Molecule. *Süleyman Demirel Üniversitesi Fen Bilimleri Enstitüsü Dergisi*. 2018; 22(1): p. 107-120.
- [30] Erganlı C.C, and Koşar B. Investigation of Physical and Chemical Properties of 2-[(2-hydroxy-4-nitrophenyl)aminomethylene]-Cyclohexa-3,5-Dien-1(2h)-One By DFT Method. *Journal of Science and Technology of Dumlupınar University*. 2016(2015 Özel Sayısı); p. 109-126.
- [31] Bhuiyan M.D.H, et al. Synthesis, linear & non linear optical (NLO) properties of some indoline based chromophores. *Dyes and Pigments*. 2011; 89(2): p. 177-187.
- [32] Kuş N, and Ilican S. 4-Florobenzil Alkolün Konformasyon ve Orbital Etkileşimlerinin DFT Metodu ile Teorik Çalışması. *Süleyman Demirel Üniversitesi Fen Bilimleri Enstitüsü Dergisi*. 2019; 23(3): p. 797-804.
- [33] Sebastian S. and Sundarag N. The spectroscopic (FT-IR, FT-IR gas phase, FT-Raman and UV) and NBO analysis of 4-Hydroxypiperidine by density functional method. *Spectrochimica Acta Part A: Molecular and Biomolecular Spectroscopy*. 2010; 75(3): p. 941-952.